BIOTECHNOLOGICAL PRODUCTS AND PROCESS ENGINEERING

Submerged culture process for biomass and exopolysaccharide production by Antarctic yeast: some engineering considerations

Serafim Vlaev · Sneghana Rusinova-Videva ·
Konstantsa Pavlova · Margarita Kuncheva ·
Ivan Panchev · Svoboda Dobreva

Abstract Production of biomass and extracellular polysaccharide (EPS) from psychrophilic *Sporobolomyces salmonicolor* AL$_1$ in a stirred bioreactor was studied. The aspects of production technical-scale parameters, namely, bioreactor flow field, biomass and EPS production rates, oxygen mass transfer per input power, as well as important product properties, such as rheology and stability of EPS mixtures, were considered. The bioprocess was found to proceed in non-Newtonian flow with consistency coefficient rising typically to 0.03 Pa.s^n and flow index declining to 0.7. Flow modeling was carried out and showed good homogenization for substrate delivery at agitation rates exceeding 400 rpm. Agitation rates lower than 400 rpm were considered counterproductive due to flow field non-uniformity. The cell density reached 5 g/l and EPS production yield reached 5.5 g/l at production rate 0.057 g EPS/l per hour (0.01 g EPS/g biomass per hour). Oxygen uptake rate and oxygen transfer rate were in the range of 0.5–1.7 mmolO$_2$/l per hour and 2–4.7 mmolO$_2$/l per hour, respectively. The mass transfer coefficient at reaction conditions was found to be in the range $K_La \sim 0.004 \sim 0.01 s^{-1}$. The bioprocess biological performance was higher at moderate agitation speed and revealed biomass diminution and cell inactivation by increasing impeller revolutions and shear rate. The product EPS was found to introduce shear-thinning behavior in water solutions with apparent viscosity of up to 30 mPa.s and to stabilize 1–2 % oil-in-water emulsions improving their lipophilic properties. The emulsion dispersion index was found to be comparable with the one of *Arlacel* 165, the emulsifier used in cosmetic. The long-term performance of the complex cream mixtures of the glucomannan prepared in commercial format was found promising for further application.

Keywords Exopolysaccharides (EPS) · Glucomannan · *Sporobolomyces salmonicolor* AL$_1$ · Bioreactor performance characteristics · EPS hydrocolloidal properties

S. Vlaev (✉)
Institute of Chemical Engineering, Bulgarian Academy of Sciences, Acad. G. Bonchev Bl. 103,
1113 Sofia, Bulgaria
e-mail: mixreac@gmail.com

S. Rusinova-Videva · K. Pavlova
Institute of Microbiology, Bulgarian Academy of Sciences,
Acad. G. Bonchev Bl. 25,
1113 Sofia, Bulgaria

M. Kuncheva · I. Panchev
University of Food Technologies, 26, Maritsa Blvrd,
4002 Plovdiv, Bulgaria

S. Dobreva
Body D Cosmetics Co, 9, Z. Stoyanov Str,
4002 Plovdiv, Bulgaria

Introduction

Exopolysaccharide (EPS) production is important resource of "green" chemistry, insofar as it supplies food, pharmaceutical industry, and cosmetics with specific molecules of valuable properties. In view of potential commercial applications, EPS biotechnology development requires information on the process performance characteristics in bioreactors that duplicate operation at technical level.

Overview of the literature uncovers several studies on the practical aspects related to the topic (Amanullah et al. 2004; Freitas et al. 2011). However, apart from the well-known detailed reports on xanthan gum production (Galindo 1994; Garcia-Ochoa et al. 2000), the studies related to new polysaccharides prevailingly miss estimates important for

implementation, such as hydrodynamic and oxygen mass transfer parameters.

Studies have focused primarily on extension of the range of EPS and its properties. Fucose-containing EPS (Torres et al. 2011) and *Ganoderma* polysaccharides (Tang et al. 2011), in parallel to hyaluronic acid (Liu et al. 2009), glucan (Crognale et al. 2007), and also others (Freitas et al. 2011) have been reported as practical goals. Product properties have been studied. Improving the hydro-balance, the rheology, and the stability behavior of commercial emulsions were developing issues (Martinez-Checa et al. 2007; Freitas et al. 2009, 2011; Rodriguez-Carmona and Villaverde 2010; Masson 2010; Zhao et al. 2012). Various strain producers have been involved, and recent studies include also extremophilic strain producer candidates (Nicolaus et al. 2010). EPS obtained from bacterial strain producers cultivated in hypersaline marine habitats (Poli et al. 2010), in volcanic areas (Romano et al. 2005), as well as from geothermal hot springs (Kambourova et al. 2009) have been analyzed. Attention has been paid also to the Antarctic ecosystem, its diversity and specific metabolism, as well as to the possibilities for application of these microorganisms to produce biologically active substances—enzymes, polysaccharides, carotenoids (Scorzeti et al. 2000; Nakagawa et al. 2004; Pavlova et al. 2004; Dimitrova et al. 2010). Little is known about EPS production by psychrophilic microorganisms. Recently, the psychrophilic yeast *Sporobolomyces salmonicolor* AL$_1$ was isolated as fertile EPS producer (Pavlova et al. 2004), and its biomass was reported to contain important antioxidants and bioactive lipids (Dimitrova et al. 2012). The aim of the present study was to reveal the EPS production scale-up parameters and product properties in view of the bioprocess further application.

Referring to previous reports (Galindo 1994; Garcia-Ochoa et al. 2000; Amanullah et al. 2004), the aspects of reaction engineering analysis important for the highly viscous EPS production are flow non-ideality (affecting substrate homogenization and supply rate) and oxygen mass transfer. These issues were studied in relation to the bioreaction evolution.

Materials and methods

Experimental vessel set-up

A scale-down version of the reactor is visualized in Figs. 2 and 3. A 5-l stirred vessel with diameter $T=0.157$ m in dual-impeller configuration with impeller diameter $D=0.064$ m (*Sartorius Biostat Aplus*) was employed. The fluid volume was $V=4.5$ l. A conventional six flat-blade turbine was the principal impeller. Air was fed through a ring sparger at rate

1 v/v/m. Oxygen and pH probes (*Hamilton, Bonaduz AG, Swiss made*) were immersed in the liquid. All operational parameters were monitored continuously on-line (*BioPAT®MFCS/DA*3.0).

Strain and culture media

Microorganism

The yeast strain *S. salmonicolor* AL$_1$ was isolated from soil in the region of the Bulgarian base on Livingston Island, Antarctica. It has been identified and registered in the National Bank for Industrial Microorganism and Cell Culture, Bulgaria, entry N 8290.

Media and growth conditions

The fermentation medium contained (g/l): sucrose, 50; $(NH_4)_2SO_4$, 2.5; KH_2PO_4, 1.0; $MgSO_4.7H_2O$, 0.5; NaCl, 0.01 %; $CaCl_2.2H_2O$, 0.01; and yeast extract, 1.0. The inoculum (10 %*w/v*) was obtained in 500 ml flasks containing 50 ml of Sabouraud medium (Merck, Germany). Previous morphological–physiological identification of the microorganism proved maximum cell growth at temperature limit 25 °C; high production of biologically active substances was obtained at 22 °C and pH 5.3. Batch fermentation for 96 h at 22 °C and initial pH 5.3 was carried out in this study.

Analytical techniques

The biomass and the amount of yeast polysaccharide were determined by dry-weight measurements. The residual sugar concentration was measured by the Megazyme method, K-SUFRG 12/05 (Megazyme 2005).

Characterization of bioreactor performance

The flow-mixing regime and the oxygen mass transfer rates were studied. Computational fluid dynamics (CFD) simulation and unsteady measurement of oxygen uptake rate (OUR), oxygen transfer rate (OTR), and gas–liquid mass transfer coefficient (K_La) were performed. In order to become amenable for scaling-up, these parameters were correlated with the stirred vessel specific input power P/V. The power, P was determined by reference to the power number for the conventional six flat-blade impeller employed (Amanullah et al. 2004) at fluid density 1,018 kg/m^3.

Fluid flow field analysis

The *rheology of the culture* broth was measured. A coaxial cylinder rotational viscometer Rheotest 2 (Germany) was

used. Measurements were carried out at 22 °C by using measuring cylinders intended for shear rates $1.5 \leq \dot{\gamma} \leq 1312\, s^{-1}$. Regression analysis of the experimental data was performed via the least squares method using a *RHEOTEST* PC program and power law approximation.

Flow non-ideality was studied. Computational simulation and visualization using Navier–Stokes models and CFD technique (Ranade 2003) were employed. The computational grids ($\sim 5.10^5$ cells) and the governing mass and momentum conservation equations were resolved by commercial codes (*ANSYS FLUENT Release 13.0, ANSYS, Inc., 2010*). The multiple reference frame approach was used for the rotating parts, and the mixture two-phase model was used in the flow simulations. The gas-phase not exceeding 8 %, a quasi-homogeneous fluid was assumed enough to show inhomogeneities in the batch. Model validity was checked at similar power law conditions (Vlaev et al. 2006). The spatial distribution of flow variables was determined.

Oxygen mass transfer analysis

$K_L a$, OUR, and OTR were determined by the unsteady stopgassing measurement technique (Garcia-Ochoa et al. 2000). Oxygen probe Ingold was used, and the dynamic measurement was conducted in line with the probe dynamics (Vlaev and Valeva 1989). OUR was determined from the depletion of dissolved oxygen (DO) concentration following interruption of the air flow and the occurrence of net respiration (r). The air flow interruption produced zero gas hold-up and zero interfacial area ($K_L a = 0$), while DO concentration C_o never decreased to zero, thus avoiding cell deterioration. It was formulated as

$$(dC_O/dt)_r = \text{OUR} \tag{1}$$

At air flow restart and known OUR, $K_L a$ and OTR were determined from the overall oxygen balance of the absorption stage (a) following integration of equation

$$
\begin{aligned}
(dC_O/dt)_a &= \text{OTR} - \text{OUR} \\
&= \mathrm{K_L a}\left(\mathrm{C_O^*} - \mathrm{C_O}\right) - \text{OUR}
\end{aligned}
\tag{2}
$$

where $(dC_O/dt)_a$ is the accumulation of oxygen in the liquid phase and C_O^* is its equilibrium value.

EPS product recovery and characterization

The biomass was isolated from the culture medium by centrifugation at $4,000 \times g$. The supernatant was treated with 96 % ethanol to obtain the polysaccharide. Laboratory details have been reported previously (Pavlova et al. 2004). The biomass was found to contain antioxidants and bioactive lipids. The EPS product was found to contain prevailingly glucomannan,

as follows (percent): carbohydrates, 90.2 ± 1.9, including mannose, 54.1, glucose, 42.6 and fucose, 3.3; additionally, proteins, 5.3 ± 0.25 and ash, 4.5 ± 3.0.

In view of using the polysaccharide as thickener and stabilizer in cosmetic mixtures, the rheology of aqueous solutions and the stability of oil-in-water emulsions containing the polysaccharide, as well as its water-sorption capacity were studied.

The *rheological parameters* of EPS water solutions were carried out according to the steady measurement technique described above (Brummer 2006).

The *emulsion stability* and the structure of emulsions containing the synthesized biopolymer were examined. Model emulsions of the type oil-in-water (o/w) containing the polysaccharide were prepared. Sunflower oil was used as a commercially available product, and 50 % was the portion of oil. Polysaccharide concentrations (in percent) 0.5; 1.0; 1.5; 2.0; and 2.5 with respect to the aqueous phase were prepared. The homogenization was carried out by homogenizer POLYTRON (*Kinematica GmbH, Kriens-Luzern, Switzerland*). The stability of the emulsion was assessed by its behavior following centrifugation carried out for 20 min at speed 50 rotations per second. The amounts of separated oil and water and the amount of the stable emulsion were measured. The quality of the resultant emulsion was registered by emulsification index and by dispersity index. The emulsification index indicated as E (%) was defined as percent height of the stable emulsion to the total fluid layer height, as reported previously by Yun and Park (2003). A dispersity index was defined as inverse translucence T (percent), and translucence was determined as an estimate of the dispersion structure, e.g., particle size. Low T revealed fine dispersion structure and stable system, while high T revealed coarse particles and unstable dispersion. In this study, T was measured by Shimadzu spectrophotometer (*UV/VIS*-12404, *Japan*) at wave length $\lambda = 540$ nm.

The glucomannan *interaction with water* was studied. The EPS involvement in colloidal dispersion systems is generally water-based, and hence its interaction with water is important. The EPS equilibrium moisture was determined. The static gravimetric method (Wolf et al. 1985) using saturated water solutions of LiCl, CH_3COOK, $MgCl_2$, K_2CO_3, $Mg(NO_3)_2$, $SrCl_2$, NaBr, NaCl, KCl, and $BaCl_2$ with known water activity (a_w) was employed. The EPS samples were placed in glass vessels over the saturated solution at constant temperature of 20 °C. The sorption isotherms of the polysaccharide were measured, and the constants of BET Eq. (3) were determined by interpolation:

$$\frac{1}{X_w} \cdot \frac{a_w}{1 - a_w} = \frac{1}{X_{w,a} \cdot B} + \frac{B-1}{X_{w,a} \cdot B} \cdot a_w \tag{3}$$

where X_w is the overall moisture content, $X_{w,a}$ is the mono-layer moisture content in grams per gram dry matter, a_w stands for water activity, and B is the BET constant.

The product's *effect on the performance behavior of cosmetic mixtures*, i.e., in presence of various components of cosmetic emulsions was examined. Viscous cream-like emulsions were prepared: The oily components were melted at 75 °C and stirred until homogeneous and water phase was heated to 75 °C and added to the oily phase, while stirring. The emulsion was homogenized by using "Ultra-Turrax" homogenizer for 1–2 min. Under moderate agitation, the emulsion was allowed to cool to 35 °C, and the preservative was added. The emulsion were stored at −10 °C for 1 month, at 45 °C for 3 months, and in a cycle of (24 h at −10 °C)/(24 h at + 45 °C) for 10 days. Two sample mixtures were prepared—a mixture with 7 % Glyceryl Stearate PEG-100 Stearate (*Arlacel* 165), and alternatively a mixture with 2 % Glucomannan (GM) bioproduct—termed sample 1 and sample 2, respectively. The ingredients of both emulsions and their concentrations were as follows (percent): cetylalcohol, 2; caryl-caprilic triglyceride, 3; paraffinum liquidum, 8; *Helianthus annuus*, 4; decyl oleate, 3.0; BHT, 0.03; methylparaben, 0.2; propylparaben, 0.1; glycerin, 3; 2-bromo-2-nitropropane-1,3-diol, 0.05; water, to 100. A stability test (Brummer 2006) consisting of visualization and sensing with positive/negative response was accomplished.

Results

Rheological parameters of the culture broth

The rheological parameters of the culture fluid were measured. As expected in polymer presence, the fluid dynamics was found to be shear-dependent. Figure 1 contains the measurement results. Preliminary measurement of cell-free and cell-loaded culture broth showed that insofar as the polysaccharide was the shear-active component, the biomass did not affect the rheological behavior. Therefore, the cell-free broth characteristics were measured. The rheological data conformed to the power law model and shear-thinning fluid rheology. Parallel to the product (P) generation dynamics, the time variation of the broth apparent viscosity and its corresponding parameters K and n was followed. They are plotted in Fig. 1a, b, respectively. The data are representative for impeller mixing at 400 and 600 rpm. As seen by the product generation dashed line, the rheological properties were in line with the amount of glucomannan (P) produced. In the study, apparent viscosity reached values of up to 13 mPa.s. Figure 1 shows the range of variation of parameters K and n and the standard error (SE). The fluid consistency coefficient K increased between 0.001 and 0.03 Pa.s^n, while the flow index n decreased

between 1 and 0.7. Typical values were $K \sim 0.026$ Pa.s^n and $n \sim 0.78$.

Following the bioreaction evolution, three states of a batch fluid were marked as characteristic for the flow field behavior. In Fig. 1a, they are indicated by L, M, and N. The three cases correspond to start-up (**L**), end of exponential growth phase (**M**), and stationary growth phase with high product concentration (**N**). The corresponding rheological parameters of the broth in terms of average shear rate at 400 rpm were: Newtonian (**L**) $K=0.001$ Pa.s^n, $n=1$, with viscosity $\mu \approx 1$ mPa.s at start-up time, and non-Newtonian (**M**) $K=0.003$ Pa.s^n, $n=0.95$ with apparent viscosity $\mu_a \approx 2.5$ mPa.s at time 30–40 h, and non-Newtonian (**N**) $K=0.026$ Pa.s^n, $n=0.78$ with $\mu_a \approx 9$ mPa.s at time 70–80 h.

Bioprocess flow field results

Flow non-ideality is important for: (1) conversion at scale-up, since often the uncontrolled factor in scale-up is the magnitude of flow non-ideality, and (2) evaluation of mass transfer, insofar as the flow field determines the type of flow model that should be employed in calculations. Consequently, the bioreactor flow field was studied.

The stirred vessel velocity field was examined and its uniformity was assessed. The simulation results are shown in Figs. 2 and 3. Inhomogeneity of the velocity field was registered. Well-mixed zones were marked off zones with hindered mixing, the first being assigned to velocity $U > 0.1U^*$, and the second to U approaching $0.01U^*$ (U^* is impeller tip velocity corresponding to impeller diameter D and speed N, $U^* = \pi N D$). The zones of low velocity of 1–5 % of U^*, and less were foreseen as problematic areas for substrate delivery. The hydrodynamics of these zones was considered.

Referring to the viscosity profile in Fig. 1a, batch **N** was regarded as a problematic one for the specific yeast fermentation due to its high consistency. Therefore, the velocity field of batch **N** was determined.

Figure 2a shows the local velocity distribution corresponding to batch **N** at moderate speed $N=300$ rpm ($U^* \approx 1$ m/s). Figure 2b shows the distribution of local apparent viscosity corresponding to the case. In the figure, the three zone types are observed and indicated as zones alpha, beta, and gamma corresponding to high, moderate, and low fluid velocity (or mobility) level. The mean velocity values and viscosity levels in the zones are indicated, respectively. According to the accepted criteria, one could observe that zones γ are the negative ones for homogenization and cells in these zones might be exposed to low rates of substrate delivery. It is seen that in region γ viscosity is reaching 13 mPa.s and velocity is lower than 10 %U^*. The flow regime conforms to incomplete mixing.
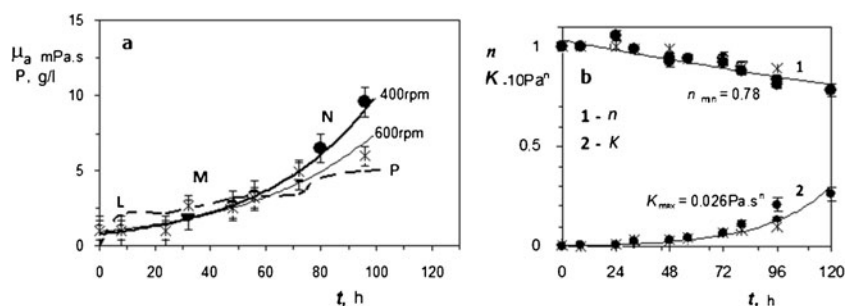
Fig. 1 **a** Broth apparent viscosity (μ_a) and polysaccharide (P) concentration versus time. Fluid states L, M, and N corresponding to start-up, exponential, and stationary cell growth, are indicated. **b** Variation of rheological constants n (curve 1) and K (curve 2) versus time. (The SE of 10 % for μ_a, 15 % for K, and 2 % for n are indicated)

The homogenization study was continued by flow field simulation at increasing impeller speed. Figure 3 presents the mixing results. 2-D velocity contour plots at various mixing intensity are compared. By increasing the agitation speed, one could observe the region of incomplete mixing (γ) to diminish and disappear, while zones α and β expand and start to prevail. The impeller revolutions of 400 rpm can be considered as starting performance that ensure complete mixing.

In order to assess the quality of mixing at various mixing intensity, the surface area ΔS difference between the areas of iso-surfaces $0.01 U^*$(m/s) and $0.1 U^*$m/s, e.g., the 3-D surfaces limiting the dark blue regions in Fig. 3a were determined and compared with the bioreactor volume-average velocity obtained. Figure 3a contains the contour plots and the ΔS values corresponding to impeller speed 100–500 rpm. Correspondingly, Fig. 3b shows the evolution of the bulk volume-average velocity versus agitation speed. As seen in Fig. 3a, the area of

iso-surfaces $0.1 U^*$m/s expanded, while the value of zonal area difference ΔS diminished. Figure 3b shows that starting from 300 rpm the mean velocity in the bulk region, i.e., the region apart from the impeller zone is exceeding the value assumed for low mobility. One could expect complete mixing to occur starting up from 300 rpm. In this study, we assumed impeller revolutions 400 rpm as the starting mixing intensity for good homogenization.

Growth and EPS production

Three levels of agitation speed were examined, 400, 500, and 600 rpm. They corresponded to specific power inputs 0.7, 1.4, and 2.4 W/l, respectively (industrial reactors operate at 1 kW/m³, thus, 1 W/l was the parameter conventional level). Aeration rate was kept at the optimum level of 4.5 l/min (1 l/min per liter bioreactor volume) established in previous laboratory studies (Pavlova et al. 2004).
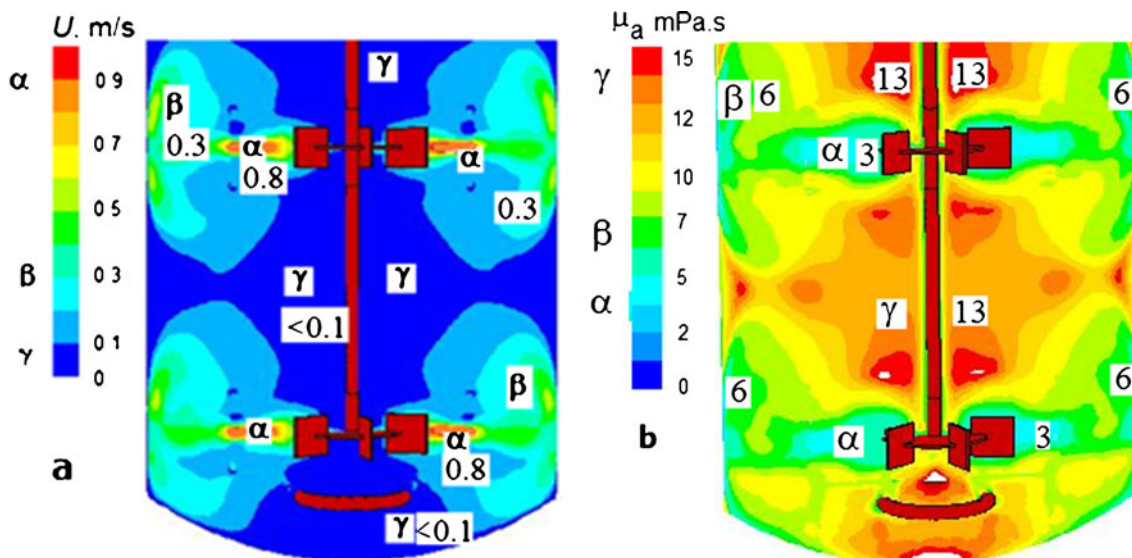

Fig. 2 Homogenization patterns in viscous batch **N** of the yeast *S. salmonicolor* AL₁. Contour plots in central plane $x=y$ at $N=300$ rpm ($K=0.026$ Pa.s^n, $\mu_a=10$ mPa.s). **a** Distribution of fluid linear velocity U zones α, β, and γ. **b** Distribution of biofluid apparent viscosity μ_a—zones α, β, and γ
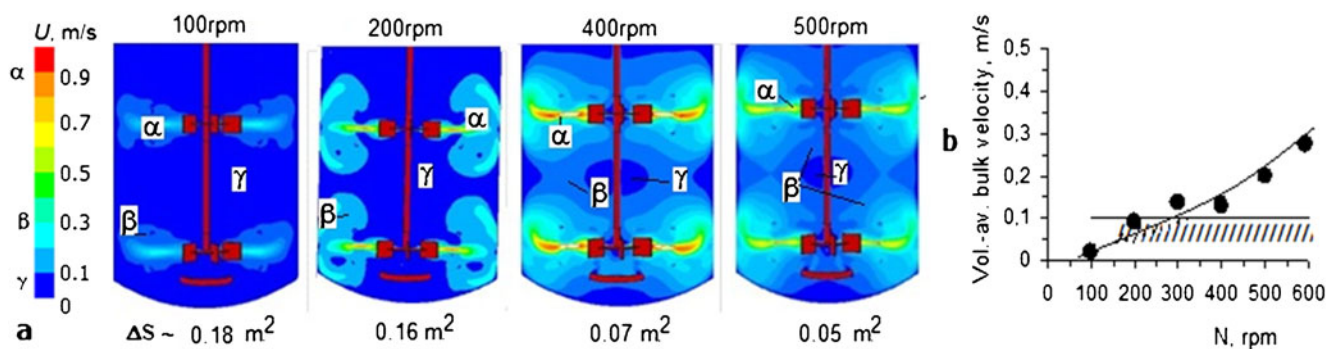
Fig. 3 **a** Homogenization mixing patterns vs. impeller speed N. **b** Volume-average velocity vs. N. The critical range of $\overline{U} < 0.1$ m/s is indicated

The kinetic plots are illustrated in Fig. 4a through Fig. 4d. The polymer biosynthesis was growth-related and intensified in the first 24 h of the bioreaction corresponding to the exponential phase of fermentation. It reached the highest level by the beginning of the stationary phase of biomass growth (fermentation time 70 h). Maximum glucomannan production of about 5 g/L was observed following the 70th hour, then in cases the biopolymer content would decrease slightly. Sucrose

assimilation was observed. It was found that *S. salmonicolor* AL$_1$ was most productive in 5.0 % sucrose-containing medium what is the case corresponding to Fig. 4. Complete assimilation occurred within 72 h (Fig. 4c).

Typical feature of the formation of EPS by yeast is the significant pH change that proves to be a regulating factor in their biosynthesis (Adami and Cavazzoni 1990). In the course of its metabolism, the *S. salmonicolor* AL$_1$ strain
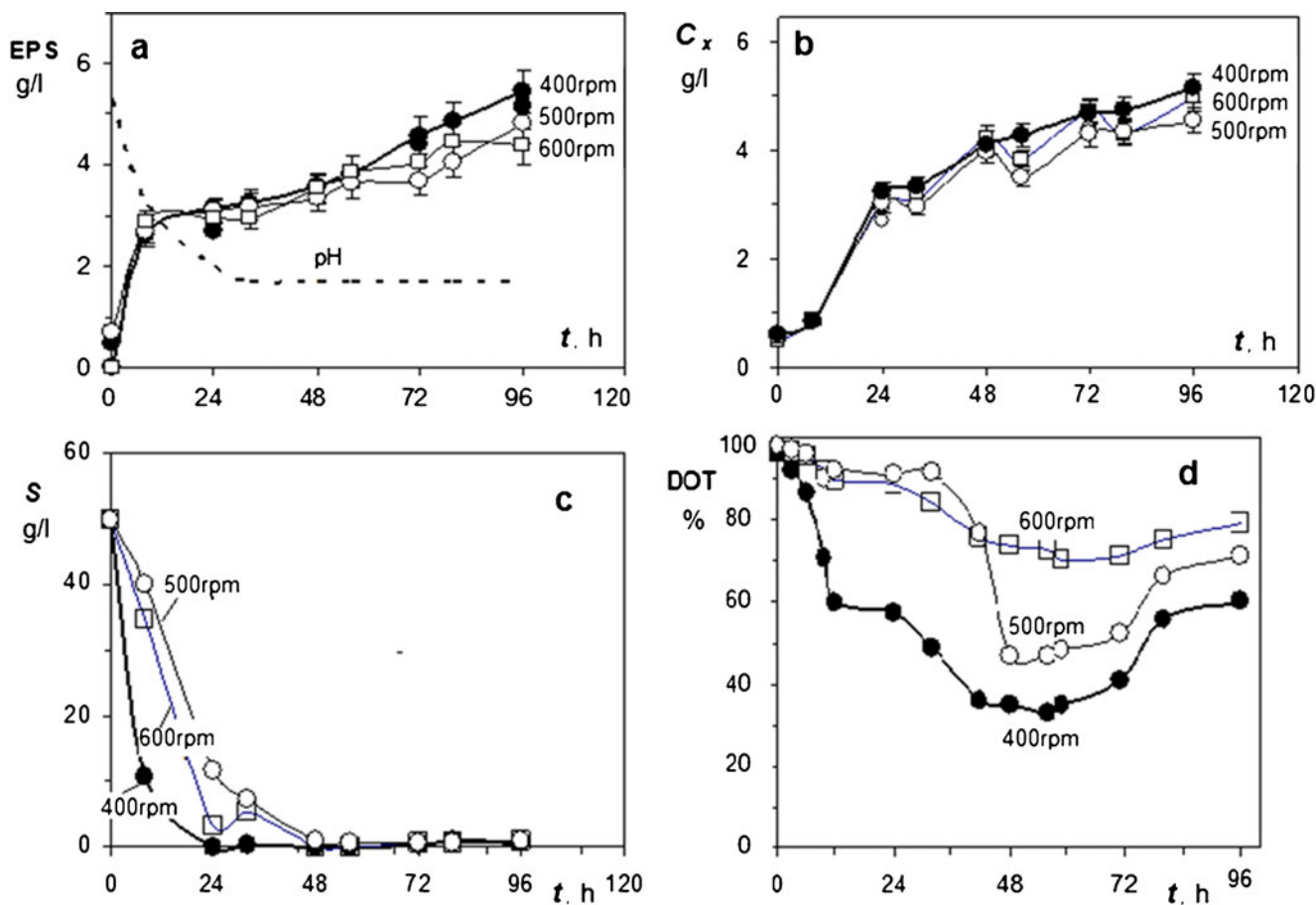

Fig. 4 Biological performance of *S. salmonicolor* strain AL$_1$ during biosynthesis of EPS in bioreactor 4.5 l. The bioprocess at 400 rpm (*filled circle*), 500 rpm (*empty circle*), and 600 rpm (*empty square*). **a**

Product EPS, **b** biomass C_x, **c** substrate S, **d** dissolved oxygen tension (DOT) (SE 8 % for EPS and 5 % for C_x is indicated)

changed the culture medium pH from the initial pH 5.3 to final pH 1.7–2.0 after 24 h, and these pH values were preserved until the bioreaction end (Fig. 4a). Thus, the polysaccharide biosynthesis took place at low pH value.

Oxygen mass transfer

The overall dissolved oxygen (DO) tension (DOT) experienced by the cells at various agitation rate is plotted in Fig. 4d. The dissolved oxygen profiles reveal different conditions of oxygen uptake. This observation showed the importance of oxygen transfer as a scaling variable. In order to be able to extrapolate the result to a larger scale, OUR, K_La, and OTR were determined. The condition of complete mixing experienced at impeller speed 400–600 rpm was utilized. OUR, K_La, and OTR values corresponding to different mixing regimes (N) and specific input power (P/V) are plotted in Fig. 5.

Evaluation of EPS properties

The rheological parameters of EPS aqueous solutions and the stability of oil-in-water emulsions containing the glucomannan, as well as its water-sorption capacity are summarized in Fig. 6.

The rheological behavior of the EPS aqueous colloidal dispersion is illustrated in Fig. 6a. In view of the biopolymer presence, the typical flow curve of the product solution shows pseudoplastic behavior (not illustrated) and conforms to the non-Newtonian power law $\tau = K\dot{\gamma}^n$, where τ is shear stress, K is consistency coefficient, $\dot{\gamma}$ is shear rate, and n stands for flow behavior index. Various concentrations were studied in the practically important concentration range between 0.5 % and 2.5 % (vol.) and the experiments produced K values in the range of 0–2 Pa.s^n and flow index in the range of 1–0.5. Based on these data, the apparent viscosity of the solutions corresponding to fixed shear rates was determined.

The glucomannan effect on emulsion stability is shown in Fig. 6, c. Figure 6b presents the relationship of lipid emulsion-forming and stabilizing effect versus polysaccharide concentration. Apart from case 1 (sample 1) of 0.5 % glucomannan, the glucomannan of higher concentrations produced by yeast *S. salmonicolor* AL$_1$ proved to possess 100 %

emulsion-forming and emulsion-stabilizing capacity for sunflower oil. One could observe that the emulsions exhibited stable appearances. The oil phase was tightly bound and the collected oil did not exceed 6 %. In fact, oil and water of 6 % and 20 %, respectively, were collected only from sample 1 corresponding to the lowest glucomannan concentration. All other emulsions remained undestroyed (Fig. 6b).

Figure 6c presents the relationship of the emulsions dispersity index (1/T) viewed as translucence T (percent) on polysaccharide concentration. Emulsions stabilized alternatively by glucomannan and emulsifier *Arlacel 165* are illustrated. It is noteworthy that high T means low dispersity and stability of the emulsion. In the figure, emulsion translucence decreased (and dispersity increased) with increase of polysaccharide concentration. The better result was in favor of the high (2 %) glucomannan concentrations. It was observed that T tended to 20 %, as the glucomannan concentration approached 2.5 % and that emulsions with 2 % and 2.5 % glucomannan and *Arlacel* showed comparable values.

The water-sorption capacity result is shown in Fig. 6d. The figure illustrates the typical water-sorption isotherm obtained for the glucomannan produced by *S. salmonicolor* AL$_1$, as well as its corresponding water-sorption parameters $X_{w,a}$ and B. It is seen that the water-sorption isotherm of the product is a sigmoidal one. The isotherm model equation (5) with $X_{w,a}$ and B constants fitted the experimental data with a correlation factor R=99.7 %. The product was classified according to the classification of Brunauer (Yun and Park 2003) as water sorbent type II. According to this classification, the values determined for the monolayer content $X_{w,a}$ and BET constant B for glucomannan show good water-sorption ability.

The effect of the glucomannan as component of cosmetic emulsions is shown in Table 1. A sample cream photomicrograph is viewed in the table. Stability performance data of samples 1–2 described in "Materials and methods" section obtained in months-long experiments are compared.

Discussion

The results of this study reveal the performance data for the specific glucomannan and its production from Antarctic yeast *S. salmonicolor* AL$_1$. Both EPS product properties

Fig. 5 Oxygen transfer parameters OUR, OTR, and K_La versus specific input power P/V during glucomannan production by *S. salmonicolor* AL$_1$. Cases M and N correspond to culture exponential and stationary growth phases, respectively (SE 20 % for OUR, 15 % for OTR, and 5 % for K_La are depicted)
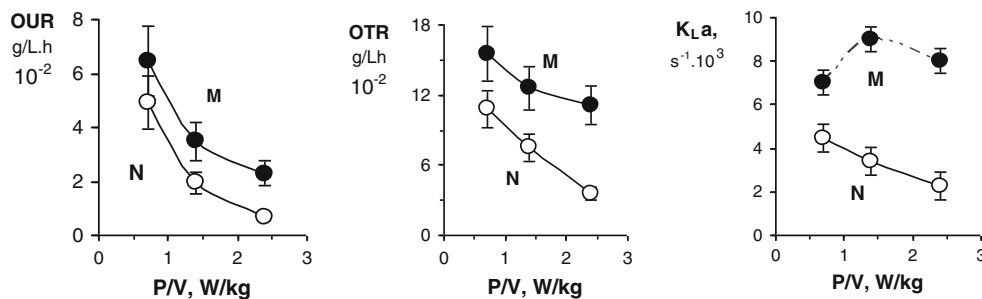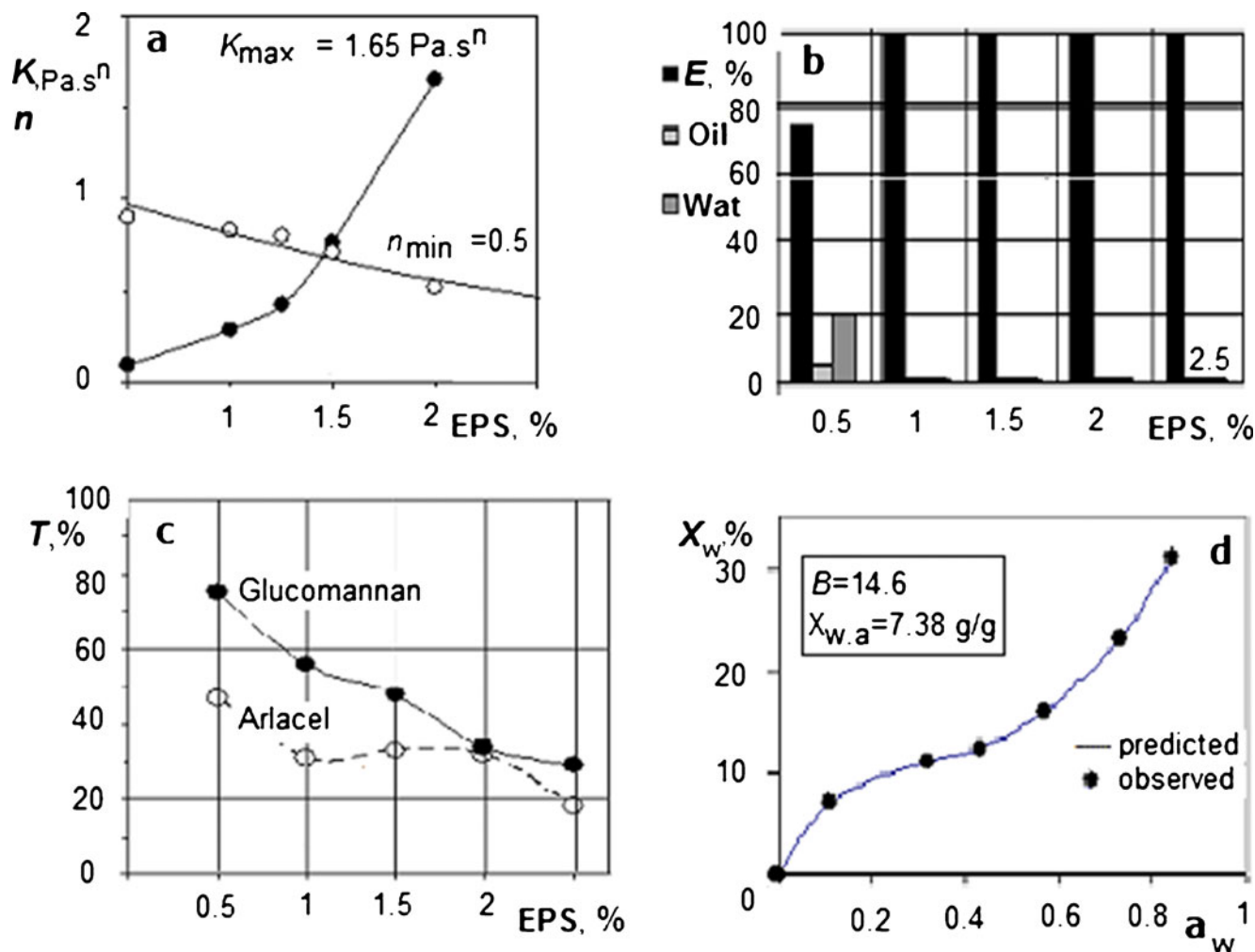
Fig. 6 Product properties. **a** The K–n domain of the glucomannan solutions. **b** Emulsifying effect (E%) of the glucomannan. **c** Translucence (T%) of EPS emulsions with 50 % oil phase. Emulsions stabilized alternatively by the glucomannan and emulsifier *Arlacel 165*. **d** Sorption isotherm of the glucomannan

and performance parameters are positive for implementation of the process. The following properties characterize the process as prospective for application.

Compared to sorption classifications (Yun and Park 2003), the values determined for the monolayer water content $X_{w,a}$ and BET constant B of the sample product (Fig. 6d) show

Table 1 Stability test of viscous emulsions under different storage conditions

	Storage temperature (°C)											
	−10 °C[a]			22 °C[a]			45 °C[a]			Cycle[b] −10 °C/45 °C		
	Readings taken in days:											
No. of sample	18	30	60	18	30	60	18	30	60	18	30	60
Sample 1 Cream with 7 % Arlacel 165	+++	+++	+++	+++	+++	+++	+++	+++	+++	+++	+++	+++
Sample 2 Cream with 2 % GM	+++	+++	+++	+++	+++	+++	+++	+++	+++	+++	+++	+++

+++ Smooth structure

[a] Duration of storage—10 days

[b] 24-h cycle storage mode over 10 days

good water-sorption ability of the specific glucomannan obtained.

It has been experienced (Brummer 2006) that in cosmetic preparations good skin perception is obtained when viscosity is 0.025–0.030 Pa.s at shear rates $\dot{\gamma} \sim 500\ s^{-1}$. In this study, the values of $n \sim 0.8$ and $K \sim 0.1\ Pa.s^n$ obtained for solutions 1–1.5 % show values of apparent viscosity 0.020–0.03 Pa.s at similar $\dot{\gamma}$ -values (i.e., $\dot{\gamma} = 500\ s^{-1}$). The flow index and the consistency obtained (Fig. 6a) characterize the yeast product as the one of high apparent viscosity and provide reasons for its application as thickener.

The dispersity of the emulsions stabilized alternatively by 2 % and 2.5 % glucomannan and emulsifier *Arlacel 165* show comparable results (Fig. 6c). Emulsions containing small amount of glucomannan exhibit good stability and dispersity of the oil phases and are competitive with the commercial emulsifier employed.

Table 1 shows that the sample cosmetic emulsions are stable in the temperature range and the time span, e.g., they were stable for 1 month at −10 °C, for 3 months at +45 °C, similarly at room temperature; no separation or any changes were observed in all samples regardless if they involve commercial emulsifier Arlacel 165 or the glucomannan of this study. Based on these results, it was inferred that the performance of glucomannan produced from *S. salmonicolor* AL_1 is favorable for preparation of cosmetic emulsions with less synthetic emulsifiers.

The bioreaction performance described in Fig. 4 shows that the bench-scale reactor kinetics are compatible with the strain selection achievement obtained previously in flasks: EPS production yield was 5.7 g/l, biomass yield was 5.5 g/l, the running EPS production volumetric rate was in the range 0.33 to 0.03 g/l per hour, and the running growth rate varied between 0.12 and 0.03 g/l per hour.

In contrast to the expected increase of EPS production at increased agitation speed (Fig. 4a), one observed production slowdown at $N=500$ and 600 rpm and specific input power exceeding 1 W/l. The effect could be explained by suppression of cells metabolic activity caused by various factors. Earlier, Gibbs and Seviour (1998) found reduction of the metabolic activity of the yeast-like *Aureobasidium pollulans* at intensive agitation. These authors assigned the effect on damage by shear. More recently, similar behavior was observed by Bandaiphet and Prasertsan (2006) with *Enterobacter*. Referring to our own experience with Antarctic yeast (Pavlova et al. 2011), *Cryptococcus laurentii* AL_{100} also languished in bioconversion at high mixing intensity. In both cases, the fact may be explained by cold-adaption of the cells at the Antarctic freezing conditions, a state in which they exhibit moderate respiration activity and are inhibited at DO over saturation. In accord with these findings, moderate mixing intensity, e.g., $N=400$ rpm at power requirement $P/V \sim 0.7$–1 W/kg for the dual-impeller bioreactor

was assumed to be a reasonable performance condition for the microorganism studied. At these conditions, specific productivity $(dP/dt.1/C_X)$ of 0.01 g EPS/g biomass per hour was obtained. This parameter compared well with the rates reported by Gibbs and Seviour (1998) for EPS production from the yeast-like *A. pollulans*, namely, 0.0117 g/g per hour and by Bandaiphet and Prasertsan (2006) for EPS production from *Enterobacter* reported as 0.04 g/g biomass per hour.

Aimed at scaling-up, the oxygen transfer parameters that ensure such productivity are important. The data in Fig. 5 could be accepted as representative controls of the biosystem behavior in response to the bioreactor performance conditions. For example in Fig. 4a, increasing agitation from 400 to 600 rpm resulted in cell performance delay; the system behavior revealed OUR decrease versus N (Fig. 5). Depending on the decreased activity of the microorganism and the decreasing DO concentration difference, OTR also decreased. The effect occurred also as increasing DO oxygen concentration in the bulk (Fig. 4d). The expected increase of K_La by increasing agitation speed is seen to be effective only partially in the exponential phase of growth and production, namely, in the case of state M (in Fig. 5). The effect seems to be balanced by some other parameter of the stationary phase (possibly surface tension and foaming). However, considering the OUR relationship with P/V, we strongly support the concept for mass transfer enhancement by the cells-activated oxygen consumption that increases the concentration gradient and displaces the reaction zone within the liquid film at the gas–liquid interphase surrounding the bubbles. At such condition, the term related to liquid film resistance, namely K_L (of K_La), would increase parallel to increasing OUR, and vice versa, would decrease with the respiration rate fall. This is clearly illustrated by the curves in Fig. 5. Similar effect on volumetric mass transfer coefficient (K_La) under oxygen consumption conditions has been observed recently by Martin et al. (2008) studying mass transfer during growth of *Trigonopsis variabilis* and *Bacillus licheniformis*. Accordingly, K_La rise caused by rising mixing intensity (P/V) is balanced by the decrease due to decrease of oxygen consumption rate OUR, as registered in Fig. 5.

In this study, the oxygen transfer parameters corresponding to EPS production with good yields and productivity were in the range OUR$\sim$0.6–1.6 mmolO$_2$/l per hour, $K_La$$\sim$0.004 − 0.01s^{-1}, OTR$\sim$2.5–4.7 mmolO$_2$/l per hour. These values are comparable with reference results reported at similar hydrodynamic conditions by Gibbs and Seviour (1998), Bandaiphet and Prasertsan (2006), and Garcia-Ochoa et al. (2000).

In conclusion, the bioprocess limiting factors and biopolymer properties of a new production process for EPS from *S. salmonicolor* AL_1 in a stirred bioreactor are

determined in view of further extrapolation to an elevated production scale. The basic characteristics of the bioprocess fluid dynamics, rheological conditions, flow field velocity structure, and dissolved oxygen transfer were revealed. The bioprocess biological performance was found to be higher at moderate agitation speed and showed biomass diminution and cells discomfort by rising impeller revolutions and shear. Agitation rates lower than 400 rpm were found counterproductive for biomass and polysaccharide due to increasing consistency. Moderate mixing intensity of 400 rpm was found to be the superior mixing regime for the bioreaction. In order to be able to scale-up the bioprocess hydrodynamics, a CFD model was formulated and applied based on the recent modeling experience with commercial codes. In order to be able to determine the mass transfer rate at various scale, it was correlated with specific power. It is demonstrated that the exoglucomannan from yeast S. salmonicolor AL$_1$ the strain producer selected from the extreme Antarctic environment is prospective for emulsion preparations. The long-term performance of complex cream mixtures of glucomannan prepared in commercial format are promising and the performance characteristics of the bioprocess can be used for extrapolation.

References

Adami A, Cavazzoni V (1990) Exopolysaccharides produced by some yeast strains. Annali di Microbiologia ed Enzimologia 40:245–253 (INIST-CNRS, Cote INIST : 5126, 35400001955542.0100)

Amanullah A, Buckland BC, Nienow AW (2004) Mixing in the fermentation and cell culture industries. In: Paul EL, Atiemo-Obeng VA, Kresta SM (eds) Handbook of industrial mixing. Wiley, New Jersey, pp 1071–1171

Bandaiphet C, Prasertsan P (2006) Effect of aeration and agitation rates and scale-up on oxygen transfer coefficient k_La in exopolysaccharide production from Enterobacter cloacae WD$_7$. Carbohydr Polym 66:216–228

Brummer R (2006) Rheology essentials of cosmetic and food emulsions. Springer-Verlag, Berlin

Crognale S, Bruno M, Moresi M, Petruccioli M (2007) Enhanced production of β-glucan from Botryosphaeria rhodina using emulsified media or fan impellers. Enzyme Microb Technol l41:111–120

Dimitrova S, Pavlova K, Lukanov L, Zagorchev P (2010) Synthesis of coenzyme Q10 and β-caroten by yeasts isolated from Antarctic soil and lichen in response to ultraviolet and visible radiations. Appl Biochem Biotechnol 162:795–804

Dimitrova S, Pavlova K, Lukanov L, Korotkova E, Petrova E, Zagorchev P, Kuncheva M (2012) Production of metabolites with antioxidant and emulsifying properties by Antarctic strain Sporobolomyces salmonicolor AL$_1$. Appl Biochem Biotechnol 169:301–311

Freitas F, Alves VD, Carvalheira M, Costa N, Oliveira R, Reis MAM (2009) Emulsifying behaviour and rheological properties of the extracellular polysaccharide produced by Pseudomonas olevorans grown on glycerol by product. Carbohydr Polym 78:549–556

Freitas F, Alves VD, Reis MAM (2011) Advances in bacterial exopolysachharides: from production to biotechnological applications. Trends Biotechnol 29:388–398

Galindo E (1994) Aspects of the process for xanthan production. Trans Inst Chem Eng 72C:227–237

Garcia-Ochoa F, Gomez Castro E, Santos VE (2000) Oxygen transfer and uptake rates during xanthan gum production. Enzyme Microb Technol 27:680–690

Gibbs PA, Seviour RJ (1998) The production of exopolysaccharides by Aureobasidium pullulans in fermenters with low-shear configurations. Appl Microbiol Biotechnol 49:168–174

Kambourova P, Mandeva R, Dimova D, Poli A, Nicolaus B, Tommonaro G (2009) Production and characterization of a microbial glucan synthesized by Geobacillus tepidamans V264 isolated from Bulgarian hot spring. Carbohydr Polym 77:338–343

Liu L, Sun J, Zhang DX, Du GC, Chen J, Xu WB (2009) Culture conditions optimization of microbial hyaluronic acid production by Streptococcus zooepidemicus. Enzyme Microb Technol 44:24–32

Martinez-Checa F, Toledo FJ, El Mabrouki K, Quesada E, Calvo C (2007) Characteristics of bioemulsifier V2–7 synthesized in culture media added of hydrocarbons: chemical composition, emulsifying activity and rheological properties. Bioresour Technol 98:3130–3135

Martin M, Montes FJ, Galan MA (2008) On the contribution of the scales of mixing to the oxygen transfer in stirred tanks. Chem Eng J 45:232–2410

Masson F (2010) Acid hyalouronique et hydratation cutanee. Ann Dermatol Venereol 137(Suppl.1):S23–S25

Megazyme.com (2005) Sucrose, D-fructose and D-glucose assay procedure. Megazyme catalogue No. K-SUFRG 12/05, Megazyme International Ireland, Bray, Ireland

Nakagawa T, Nagaoka T, Taniguchi S, Miyaji T, Tomizuka N (2004) Isolation and characterization psychrophilic yeasts producing cold adapted pectinolytic enzymes. Lett Appl Microbiol 38:383–387

Nicolaus B, Kambourova M, Oner ET (2010) Exopolysaccharides from extremophiles: from fundamentals to biotechnology. Environ Technol 31:1145–1158

Pavlova K, Koleva L, Kratchanova M, Panchev I (2004) Production and characterization of an expolysaccharide by yeast. World J Microbiol Biotechnol 20:435–439

Pavlova K, Rusinova-Videva S, Kuncheva M, Kratchanova M, Gocheva M, Dimitrova S (2011) Synthesis and characterization of an exopolysaccharide by Antarctic yeast strain Cryptococcus laurentii AL$_{100}$. Appl Biochem Biotechnol 163:1038–1052

Poli A, Anzelmo G, Nicolaus B (2010) Bacterial exopolysaccharides from extreme marine habitats: production, characterization and biological activities. Mar Drugs 8:1779–1802. doi:10.3390/md8061779

Ranade VV (2003) Computational flow modeling for chemical reactor engineering. Academic Press, San Diego

Rodriguez-Carmona E, Villaverde A (2010) Nanostructured bacterial materials for innovative medicines. Trend Microbiol 18:423–430

Romano I, Poli A, Lama A, Gambacorta A, Nicolaus B (2005) Geobacillus thermoleovorans subsp. stromboliensis subsp. nov isolated from the geothermal volcanic environment. J Gen Appl Microbiol 51:183–189

Scorzeti G, Petrescu I, Yarrow D, Fell J (2000) Cryptococcus adeliensis sp. nov., a xylanase producing basidiomycetous yeast from Antarctica. Anton Leeuw 77:153–157

Tang Y-J, Wei Z, Liu R-S, Zhu L-W, Zhong J-J (2011) Scale-up study on the fed-batch fermentation of Ganoderma lucidum for the hyperproduction of ganoderic acid and Ganoderma polysaccharides. Process Biochem 46:404–408

Torres CAV, Marques R, Antunes S, Alves VD, Sousa I, Ramos AM, Oliveira R, Freitas F, Reis MAM (2011) Kinetics of production and characterization of the fucose-containing EPS from Enterobacter A47. J Biotechnology 156:261–267

Vlaev SD, Valeva M (1989) Applicability of sterilizable oxygen electrode response characteristics to oxygen transfer dynamic measurements in bioreactors. J Biotechnology 11:83–87

Vlaev SD, Georgiev D, Nikov I, Elqotbi M (2006) Shear analysis of mixing reactors—verification of the CFD approach. In: Magelli F, Baldi G, Brucato A (eds) Proc 12th European Conf. on Mixing. AIDIC, Bologna, pp 479–486

Wolf W, Speiss WEL, Jung G (1985) Standardization of isotherm measurements. In: Simatos D, Multon JL (eds) Properties of water in foods. Martinus Nijhoff Publ, Amsterdam, pp 661–679

Yun UJ, Park HD (2003) Physical properties of an extracellular polysaccaride produced by Bacillus sp. CP912. Lett Appl Microbiol 36:282–287

Zhao L, Fan F, Wang P, Jiang X (2012) Culture medium optimization of a new bacterial extracellular polysaccharide with excellent moisture retention activity. Appl Microbiol Biotechnol DOI. doi:10.1007/s00253-012-4515-0